Polarization of Parametric X Radiation

V. V. Morokhovskii,[1] K. H. Schmidt,[2] G. Buschhorn,[2] J. Freudenberger,[1] H. Genz,[1] R. Kotthaus,[2,*] A. Richter,[1] M. Rzepka,[2] and P. M. Weinmann[2]

[1]*Institut für Kernphysik, Technische Hochschule Darmstadt, Schlossgartenstrasse 9, D-64289 Darmstadt, Germany*

[2]*Max-Planck-Institut für Physik (Werner-Heisenberg-Institut), Föhringer Ring 6, D-80805 München, Germany*

(Received 8 July 1997)

Polarization properties of parametric x radiation (PXR) produced by $E_0 = 80.5$ MeV electrons interacting with a 13 μm thick silicon crystal have been investigated. The direction and the degree of the linear polarization of PXR observed at about 20° with respect to the electron beam direction were determined by means of a novel method exploiting directional information of the photoelectric effect in a charge coupled device consisting of 6.8×6.8 μm pixels. Comparison of the results with a newly derived theoretical expression exhibits very good agreement if on top of the basic interaction process underlying PXR effects decreasing the polarization are taken into account. [S0031-9007(97)04605-X]

PACS numbers: 41.60.–m, 07.85.–m, 41.75.Ht

Parametric x radiation (PXR) is a highly monochromatic radiation produced by a relativistic charged particle traversing a crystal. It originates from the coherent superposition of the electromagnetic waves emitted due to the polarization of crystal atoms periodically distributed along the particle trajectory. For highly relativistic charged particles (Lorentz factor $\gamma = 1 + E_0/mc^2 \gg 1$) the PXR intensity is concentrated predominantly within a small angular cone well separated from the electron beam. While PXR has already been predicted about three decades ago [1], it was first observed only in 1985 [2] and has attracted considerable interest ever since. The spectral and angular properties of PXR produced by electrons mostly in silicon and diamond crystals have been studied over a large range of electron energies from a few MeV up to several GeV. For recent investigations we refer to [3–13] and references therein. In general, the experimental results are well described by a so-called kinematical theory [3].

So far the polarization character of PXR is largely unexplored. There exists only one experimental investigation [14,15] using 900 MeV electrons and a 370 μm Si crystal in which for three discrete points of the (220) reflex the linear polarization was measured. Away from the center of the reflex a high degree of polarization was found. The polarization was claimed [14] to have a radial distribution in analogy to Čerenkov radiation. Since the applied theoretical approach [16] to the data does not contain explicit relations regarding the polarization properties of PXR, the quoted agreement [14,15] between experiment and theory appears to be fortuitous. It has been the aim of the work described in the present article to determine the polarization degree and direction of PXR for experimental conditions similar as in [14,15] applying a novel experimental technique which facilitates a continuous coverage of a substantial fraction of the diffraction pattern and to derive for the first time the appropriate expressions for the observables describing the polarization properties of PXR.

Within the framework of the kinematical theory [3] it can be shown [17] that PXR is—under ideal conditions—100% linearly polarized at every single point of its angular distribution. The polarization direction, however, reveals a different behavior than stated in [14,15]. Using Eq. (19) from [3] an expression for the polarization direction can be derived, and in the ultrarelativistic limit ($v/c = 1$) the orientation of the polarization plane for every point of the diffraction pattern is given by the following axial vector [17]

$$\vec{\Psi} = \hat{k} \arctan \frac{\hat{g} \cdot [\hat{v} \times \hat{k}]}{(\hat{v} \cdot \hat{k})[\hat{g} \cdot (\hat{v} + \hat{k})]} . \qquad (1)$$

As shown in Fig. 1, $\vec{\Psi}$ measures the orientation of the polarization plane with respect to the radiation plane spanned by the photon momentum direction (unit vector

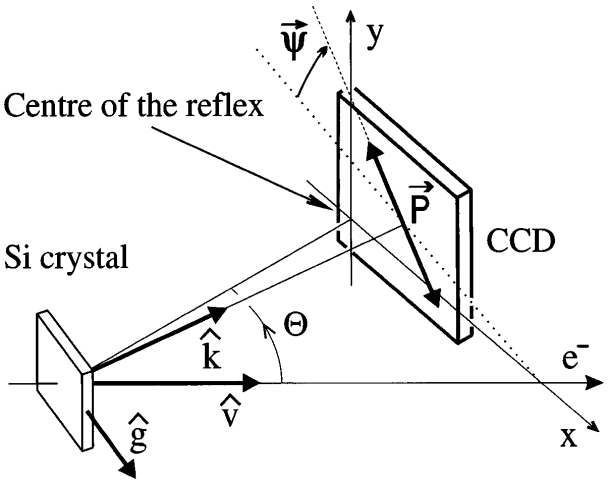

FIG. 1. Schematic view of the experimental setup and definition of variables showing the electron beam direction, the radiation producing crystal, as well as the position of the CCD polarimeter. The center of the PXR reflex is at an angle Θ to the electron beam direction (unit vector $\hat{v}$). $\vec{P}$ denotes the magnitude and the direction of the linear polarization of PXR emitted in the direction of unit vector $\hat{k}$. $\hat{k}$ and $\hat{v}$ define the radiation plane. $\hat{g}$ is the unit vector in the direction of the reciprocal lattice vector of the diffracting crystal plane.

$\hat{k}$) and the electron beam direction (unit vector $\hat{v}$) in a right-handed sense relative to the axis $\hat{k}$. The normalized reciprocal lattice vector of the diffracting crystal plane is denoted by $\hat{g}$.

Four typical angular distributions of the polarization direction resulting from Eq. (1) are shown in Fig. 2 for the angular region in the vicinity of the center of the PXR diffraction pattern ($\theta_x = 0$; $\theta_y = 0$) at observation directions $\Theta = 20°$, 90°, 135°, and 160°. Each dash indicates the polarization direction at the corresponding point of the angular distribution. In particular, Fig. 2(a) displays the angular distribution expected for the experimental conditions described below as well as for those of [14,15]. The angular region shown covers nearly the entire PXR diffraction pattern for both cases. Figure 2(a) shows that the conclusions quoted in [14,15], i.e., a radial distribution of the polarization direction, is in contradiction with our evaluations. A "hyperbolic" distribution of polarization planes like in Fig. 2(a) is expected for the observation angles in the forward hemisphere. A completely different behavior occurs in the backward hemisphere. At $\Theta = 135°$ and $\Theta = 160°$, the radial distributions shown in Figs. 2(c) and 2(d), respectively, are predicted. The special case for the PXR reflex emitted at $\Theta = 90°$ is given in Fig. 2(b).

Polarization properties of PXR were determined exploiting the photoelectric effect in a charge coupled device (CCD) detector [18,19] covering the region of the diffraction pattern marked in Fig. 2(a). The analysis of the photoelectron tracks following a $\cos^2$-distribution with respect to the electric field vector of the absorbed photon enables one to extract the degree and the orientation of the photon beam polarization in one single measurement. Simultaneously, the photon energy and position were determined with high accuracy [20], which is also important for a polarization analysis of PXR.

The experiment [20] was carried out at the Darmstadt superconducting linear electron accelerator S-DALINAC [21] with a low-emittance beam of $E_0 = 80.5$ MeV electrons ($\gamma = 158.5$) and by using a Si(100) single crystal. The crystal thickness of 13 μm results in multiple scattering of 0.9 mrad (1σ) which is of the order of the incident beam divergence of 0.5 mrad. The beam spot radius at the crystal was about 0.5 mm. The CCD detector, stabilized at an operating temperature of 20 °C , was located outside the vacuum chamber at a distance $L = 503$ mm from the Si crystal. It covered an area of 8.7×7.0 mm^2 with 1.3×10^6 square pixels of 6.8 μm each, spanning an angular region in x direction from 20° to 21°. The crystal was oriented in such a way that one quadrant of the (220) diffraction pattern was accepted (see Figs. 1–3). High precision alignment of the diffraction pattern with respect to the CCD detector is crucial for the analysis of PXR polarization properties and was facilitated by recording energetically resolved 2-dimensional PXR angular distributions by direct photon detection [20]. Figure 3 shows an image obtained by integration over a large exposure time. The PXR intensity crest lies on a circle $L/\gamma = 3.17$ mm shown by the dashed line around the intensity minimum at the center of the reflex in the origin of the x-y coordinate system. The position of the PXR minimum was determined with an accuracy of about 200 μm. From the photon energy of 17.70 ± 0.05 keV measured in the left column of bins the crystal orientation and the direction, corresponding to

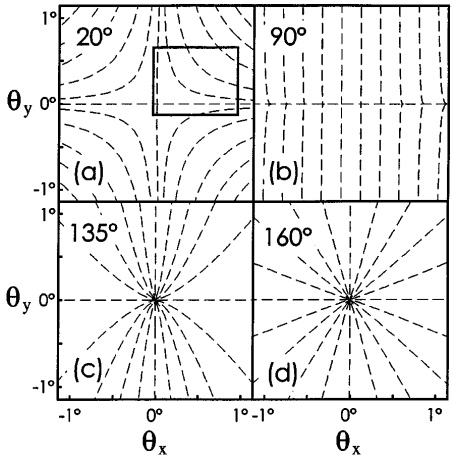

FIG. 2. Calculations of the angular distribution of the PXR polarization direction using Eq. (1) of the main text for reflexes observed at $\Theta = 20°$, 90°, 135°, and 160°. θ_x and θ_y are angular coordinates with respect to the center of the reflex. Each dash indicates the direction of the local polarization plane. The measurements were performed for the angular region in the upper right-hand quadrant of (a). The rectangle marks the polarimeter acceptance.

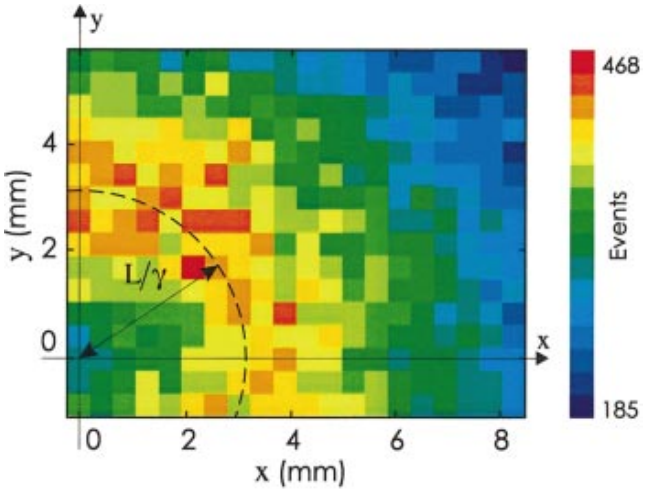

FIG. 3(color). Image of a PXR angular distribution obtained over a large exposure time. The intensity maximum follows a circle about the center of the reflex in the origin of the x-y coordinate system. The radius of the circle corresponds to a cone of opening angle $1/\gamma = 6.3$ mrad .

the center of the PXR pattern $\Theta = (20.98 \pm 0.06)°$ (see Fig. 1), were found.

For the polarization analysis the CCD was operated at a minimum static period of 10 ms between readout cycles [20]. This mode of operation integrates over the y coordinate (Fig. 3). Therefore, the PXR polarization was analyzed within rectangular stripes [labeled from 0 to 7 in Fig. 5(a) below] each 1.088 mm wide in x and extending in y over the full CCD height of 7.0 mm.

Two types of charge depositions in the CCD were exploited for photoelectron direction estimates: 2-pixel events with charge in 2 adjacent pixels and multipixel events with charge deposited in clusters of at least 3 contiguous pixels. The CCD polarimeter was calibrated using monochromatized synchrotron radiation with known polarization properties [19,20]. At energies between 17.5 and 20.0 keV, covering the PXR energy range of the present experiment, the 2-pixel (multipixel) analyzing power rises linearly from 3.0% to 4.0% (0.9% to 1.6%). Event-direction asymmetries had to be corrected for background contributions mainly due to penetrating charged particles. Energy spectra for the best and the worst cases of signal-to-background ratio are given in Fig. 4. The amount of background inside the signal region was measured directly with the Si crystal tilted into an arbitrary direction. The background polarization was determined from sidebands adjacent to the signal region. Multipixel events, despite their substantially smaller analyzing power, are more useful for polarization analyses due to their much larger abundance. Moreover, such events having a continuous angular distribution contain the full information about the direction and the degree of the linear polarization. Therefore, in the analysis presented here only multipixel events were taken into account.

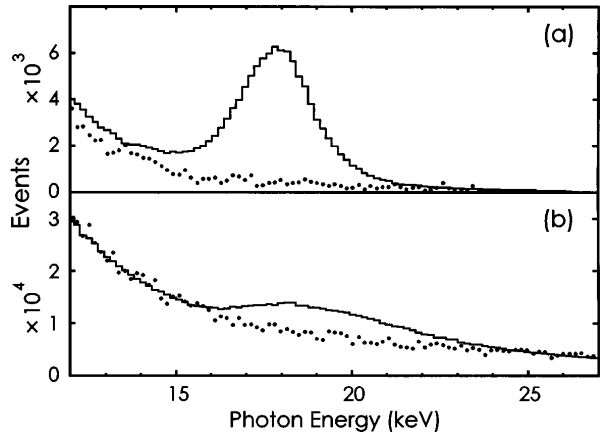

FIG. 4. PXR energy spectra obtained for the (220) reflex of a 13 μm Si crystal at an observation angle of $\Theta \approx 20°$ representing the best and the worst cases of signal-to-background ratio. (a) 2-pixel events in stripe No. 0, (b) multipixel events in stripe No. 7. The background contribution (dotted line) is determined separately with the Si crystal tilted into an arbitrary direction.

The experimental results for the integral polarization degree and the average direction within each of the eight stripes of the CCD polarimeter are displayed in Fig. 5. The direction of each arrow in Fig. 5(a) denotes the orientation of the polarization plane, while the length represents the degree of polarization. The dashed lines (as in Fig. 2) indicate the polarization direction calculated according to Eq. (1). It becomes apparent that the measured polarization direction follows a hyperbolic distribution confirming Eq. (1). The experimental points in Fig. 5(b) show the polarization direction for each polarimeter stripe. The orientation of the polarization plane thus changes from about $\Psi = 89°$ for stripe No. 0 to $\Psi = 0°$ for stripe No. 7. The measured degree of the polarization [Fig. 5(c)] is significantly less than 100% and reaches a minimum of about 50% for stripe No. 2. This reduction from 100% is mainly due to the variation of the polarization plane over the angular acceptance of each stripe [Fig. 5(a)]. The degree of polarization is further influenced by the electron beam dimension and its angular divergence, multiple electron scattering inside the

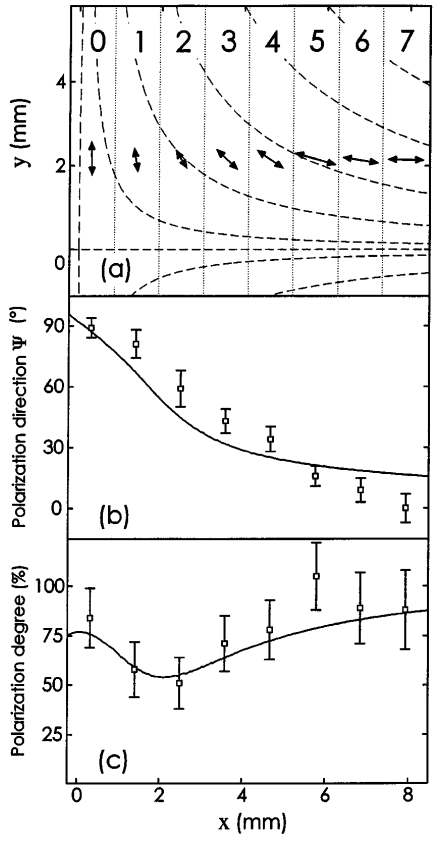

FIG. 5. Experimental results for the orientation of the polarization plane and the degree of linear polarization obtained for eight CCD polarimeter stripes denoted 0 to 7 in (a). Each arrow in (a) represents the direction and the degree of the linear polarization measured within the corresponding stripe. The dashed lines display calculated results as in Fig. 2(a). The solid lines in (b) and (c) represent the result of a Monte Carlo simulation using Eq. (1).

crystal, and crystal mosaic spread. All these effects cause a spread of $\hat{k}$, $\hat{v}$, and $\hat{g}$ in Eq. (1) with the result that the polarization direction is distributed about some average value. To compare the experimental results with the theoretical prediction a Monte Carlo simulation [17] employing Eq. (1) and taking into account simultaneously all processes mentioned above as well as the absorption of photons in the crystalline medium has been performed. As shown in Figs. 5(b) and 5(c), the results are in good agreement with the experimental findings. Electron beam parameters and multiple electron scattering decrease the polarization degree significantly only in the vicinity of the center of the PXR reflex, i.e., in stripe No. 0. The reduction of the polarization degree due to a possible crystal mosaicity of much less than 0.1 mrad is negligible.

In conclusion, it can be stated that the experimental results confirm Eq. (1) describing the polarization direction. This result is in contradiction to the interpretation of the only other existing PXR polarization measurement performed so far [14,15]. For a complete verification of the theory, polarization measurements at different observation angles need to be carried out. In particular, the completely different orientation of polarization planes for backward diffraction [Figs. 2(c) and 2(d)] should be experimentally verified. The special case of $\Theta = 90°$ [Fig. 2(b)] is of great interest for applications. The entire PXR reflex is expected to be completely polarized perpendicular to the x axis of the diffraction pattern. The effects decreasing the polarization degree mentioned above are negligible in this case.

This work has been supported by the Gottlieb Daimler and Karl Benz-Stiftung, and the German Federal Minister for education and research (BMBF) under Contract No. 06DA820. The authors wish to thank H.-D. Gräf and his crew for the expert operation of the accelerator and the technical staff of the Max-Planck-Institut für Physik for the contributions to the instrumentation. The MPI authors gratefully acknowledge the hospitality extended to them at the S-DALINAC and the generous support of detector calibration measurements given by HASYLAB at the Deutsches Elektronen-Synchrotron DESY at Hamburg.

*Corresponding author.
Electronic address: rik@mppmu.mpg.de

[1] M. L. Ter-Mikaelian, *High Energy Electromagnetic Processes in Condensed Media* (Wiley, New York, 1972), pp. 332–336.
[2] S. A. Vorob'ev, B. N. Kalinin, S. Pak, and A. P. Potylitsyn, JETP Lett. **41**, 1 (1985).
[3] H. Nitta, Phys. Lett. A **158**, 270 (1991).
[4] H. Nitta, Phys. Rev. B **45**, 7621 (1992).
[5] R. B. Fiorito *et al.*, Phys. Rev. Lett. **71**, 704 (1993).
[6] R. B. Fiorito *et al.*, Phys. Rev. E **51**, R2759 (1995).
[7] S. Asano *et al.*, Phys. Rev. Lett. **70**, 3247 (1993).
[8] I. Endo *et al.*, Phys. Rev. E **51**, 6305 (1995).
[9] J. Freudenberger *et al.*, Phys. Rev. Lett. **74**, 2487 (1995).
[10] J. Freudenberger *et al.*, Nucl. Instrum. Methods Phys. Res., Sect. B **115**, 408 (1996).
[11] J. Freudenberger *et al.*, Nucl. Instrum. Methods Phys. Res., Sect. B **119**, 123 (1996).
[12] J. Freudenberger *et al.*, Appl. Phys. Lett. **70**, 267 (1997).
[13] K.-H. Brenzinger *et al.*, Z. Phys. A **358**, 107 (1997).
[14] Yu. N. Adishchev *et al.*, JETP Lett. **48**, 342 (1988).
[15] Yu. N. Adishchev *et al.*, Nucl. Instrum. Methods Phys. Res., Sect. B **44**, 130 (1989).
[16] V. G. Baryshevsky and I. D. Feranchuk, J. Phys. (Paris) **44**, 913 (1983).
[17] V. V. Morokhovskii, Dissertation D17, Technische Hochschule Darmstadt (to be published).
[18] G. Buschhorn *et al.*, Nucl. Instrum. Methods Phys. Res., Sect. A **346**, 578 (1994).
[19] K. H. Schmidt *et al.*, Proc. SPIE **2808**, 230 (1996).
[20] K. H. Schmidt, Dissertation, Technische Universität München, 1997, Report No. MPI- PhE/97-07 (unpublished).
[21] J. Auerhammer *et al.*, Nucl. Phys. **A553**, 841c (1993).